European Journal of Computational Mechanics, 2013
Vol. 22, Nos. 2–4, 198–208, http://dx.doi.org/10.1080/17797179.2013.820979

Taylor & Francis
Taylor & Francis Group

Micromechanical approach for the behaviour of open cell foams

Y. Maalej[a]*, M.I. El Ghezal[b] and I. Doghri[b]

[a]*U2MP, University of Sfax, ENIS, University of Tunis El Manar, ENIT, BP 37, Le Belvédère, 1002, Tunis, Tunisia;* [b]*UCL, IMMC, bâtiment Euler, 4 Av. G. Lemaître, B-1348, Louvain-La-Neuve, Belgium*

The objective of this paper is the prediction of the macroscopic behaviour of open-cell foams in elasticity and viscoelasticity as function of their microstructure by using a micromechanical approach. Open cellular materials are characterised by remarkable mechanical properties with light weight. Such materials are largely used in various applications mainly in energy absorption. Polyurethane foam is used as an application once its microstructure is majorly described by an open-cell foam. Finite Element computations are performed on a unit cell subjected to periodic boundary conditions. Then, a micromechanical model based on Cosserat homogenisation framework is performed to predict the macroscopic elasticity. The linear viscoelastic behaviour is deduced from elastic results by taking advantage of correspondence principle. Finally, the results are confronted to various models developed in literature.

Keywords: open cell; micromechanics; foams; elasticity; viscoelasticity

1. Introduction

Mechanical properties of open-cell foam materials in elasticity and viscoelasticity have been widely studied in the literature. They are used in diverse areas of application such as energy absorption, soundproofing and thermal isolation. Generally, shapes of cells in foams (Figure 1(a)) are idealised by regular geometric shape such as rhombic dodecahedron, tetrakaidecahedron Zhu, Knott, and Mills (1997), Li, Gao and Roy (2003) and cubic cells for more simplicity Gibson (2005), Roberts and Garboczi (2002). The mechanical behaviour was achieved by homogenising the heterogeneous structure of the material using several approaches such as the theory of beams Zhu et al. (1997), Li et al. (2003), Mills (2006) and the semi-empirical method with fitting parameters Gibson (2005), Huang and Gibson (1991).

This paper deals with the prediction of the macroscopic behaviour of open-cell foams in elasticity and viscoelasticity as function of their microstructure. Reliable macroscopic behaviour hinges on accurate understanding of their microstructure. Polyurethane (PU) foams, considered as solid-void two-phase cellular medium, are topology-sensitive and, as a result, their mechanical performance depends on the cell micro-architecture, the relative foam density and the properties of the PU constitutive strut material. This implies that micromechanical models must incorporate microstructural features of

*Corresponding author. Email: yamen.maalej@enit.rnu.tn

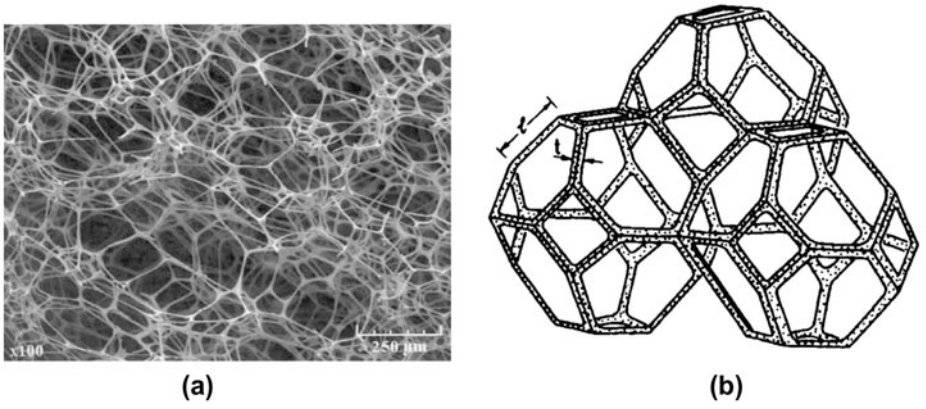

Figure 1. (a) SEM of foam microstructure; (b) Assembly of ideal tetrakaidecahedra, after Magnenet, Rahouadj, Bacher, and Cunat (2008).

cells. Figure 1(a) shows an SEM observation of a PU foam microstructure. It can be seen that the microstructure of such a foam has a three-dimensional open-cell topology and may be represented by a tetrakaidecahedron cells packed in a Body-Centred Cubic (BCC) lattice. As illustrated in Figure 1(b), the tetrakaidecahedron cell contains six square and eight hexagonal faces. It is created by truncating the corners of a cube.

Based on this microstructural description, FE model is performed on a unit cell under periodic boundary conditions. In the second part of this paper, a micromechanical model using Cosserat homogenisation framework will be conducted to predict the elastic properties and extended to viscoelasticity by taking advantage of the correspondence principle. Numerical and analytical model will be developed and assessed by comparing them to results of references.

2. Numerical model

2.1. Elasticity

Finite element simulation is performed on a tetrakaidecahedral cell sitting on a BCC lattice. As noted in the introduction, this model represents well the micro-architecture of the PU open-cell foam. Since the microstructure of this material is periodic along the three directions, a unit cell is sufficient to provide the information needed to compute the effective properties at the macroscopic scale provided that periodic boundary conditions are imposed Bornert, Bertheau and Gilormini (2001). Finite element simulations are, therefore, performed on a tetrakaidecahedral unit cell generated by Abaqus software (Figure 2(a)). The struts are modelled by Timoshenko beam elements (Abaqus type B31) having square cross sections. The relative density R is defined as the density of the cellular material divided by that of the solid from which the cell walls are made:

$$R = \frac{3A}{2\sqrt{2}L^2} \tag{1}$$

where L the length of an edge and A its cross-section area. The variation of the relative density R is performed by adjusting the beam cross-section area.

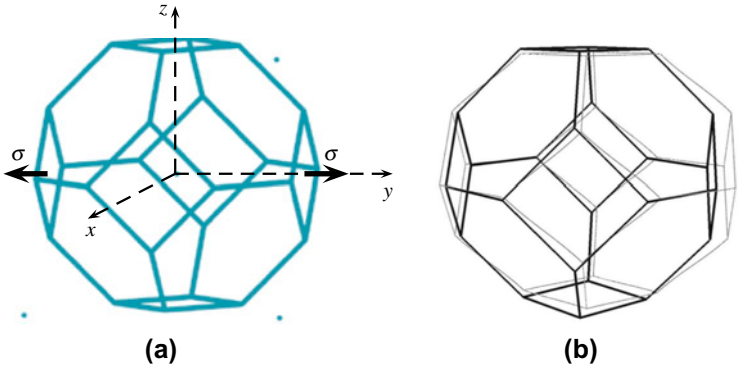

Figure 2. (a) FE model for tetrakaidecahedral unit cell; (b) Deformed shape under tensile test (thin lines).

In order to apply periodic boundary conditions, we placed the unit cell in a fictitious cube of dimensions L so that the six square faces of the tetrakaidecahedral unit cell are tangent to the faces of the cube (Figure 2(a)). The origin of the coordinate system (O, x, y, z) is placed in the centre of the cube. Next, we added a set of master $(M(-0.5L,\ -0.5L,\ -0.5L))$ and slave nodes (S_1, S_2 and S_3, respectively, of coordinates $(0.5L,\ -0.5L,\ -0.5L)$, $(-0.5L,\ 0.5L,\ -0.5L)$ and $(-0.5L,\ -0.5L,\ 0.5L)$. Periodic boundary conditions involve the following conditions on the displacement fields u:

$$\begin{aligned} u_i(M) - u_i(S_1) &= u_i(\text{nodes} \in \text{face x} = -\tfrac{L}{2}) - u_i(\text{nodes} \in \text{face x} = +\tfrac{L}{2}), \quad i \in [1,3] \\ u_i(M) - u_i(S_2) &= u_i(\text{nodes} \in \text{face y} = -\tfrac{L}{2}) - u_i(\text{nodes} \in \text{face y} = +\tfrac{L}{2}), \quad i \in [1,3] \\ u_i(M) - u_i(S_3) &= u_i(\text{nodes} \in \text{face z} = -\tfrac{L}{2}) - u_i(\text{nodes} \in \text{face z} = +\tfrac{L}{2}), \quad i \in [1,3] \end{aligned} \tag{2}$$

In order to eliminate the rigid body displacement, vector u is imposed as $u_i(M) = 0,\ \ i \in [1,3]$ (M is a fixed node), $u_3(S_2) = 0$ (no rotation around x), $u_1(S_3) = 0$ (no rotation around y) and $u_2(S_1) = 0$ (no rotation around z).

Due to the cubic symmetry, both the effective Young's modulus and Poisson's ratio can be derived from a tensile test applied along one of the cube axes. A displacement is applied to one of the slave nodes. The macroscopic stress tensor $\bar{\boldsymbol{\sigma}}$ is computed from the external tractions at the master and slave nodes and the strain tensor $\bar{\boldsymbol{\varepsilon}}$ from displacement components of these nodes (deformed shape under tensile test is presented in Figure 2(b)). Furthermore, the approach is to identify the significant terms of stress $\bar{\boldsymbol{\sigma}}$ and strain $\bar{\boldsymbol{\varepsilon}}$ tensor with those of the constitutive law.

For a PU open-cell foam, the constitutive material of the solid skeleton is considered as an isotropic solid characterised by Young's modulus $E = 100$ MPa and Poisson's ratio $v = 0.45$. Table 1 represents the variation of computed foam's Young's moduli and Poisson's ratio as function of the relative density R (1).

Table 1. Young's moduli and Poisson's ratio as function of the relative density R.

Relative density R (%)	1	2.5	5	7.5	10	14
Young's modulus (Mpa)	0.90	4.96	17.3	34.6	55.8	95.7
Poisson's ratio	0.49	0.48	0.46	0.45	0.44	0.42

2.2. Viscoelasticity

Similar to the elastic analysis, we conducted FE computations on different unit cells of cellular solids. The unit cell undergoes uniaxial compression creep. The viscoelastic strut material's stress relaxation data can be approximated by a rheological model constituted by a set of Maxwell elements (Figure 4(a)). Then, the relaxation Young's modulus $E_R(t)$ is given by a Prony series:

$$E_R(t) = E_\infty + \sum_{i=1}^{n} E_i \exp(-t/\tau_i) \tag{3}$$

where E_∞ the modulus at infinity and E_i those associated with relaxation times τ_i. As an application, we will use for this analysis, the experimental data obtained by Zhu and Mills (2006) on solid Bulpren PU. They approaximated the relaxation Young's modulus with eight relaxation times $\tau_i = 10^{\,i-3}$ of moduli $E_i = 9.3$ MPa for $i = 1$ to 8 and $E_\infty = 28$ MPa.

The FE macroscopic creep compliance $\bar{J}(t)$ can be computed using:

$$\bar{J}(t) = \bar{\varepsilon}(t)/\sigma_0 \tag{4}$$

where $\bar{\varepsilon}$ is the resulting macroscopic strain computed as detailed in Section 2.1. Figure 3 represents the macroscopic creep compliance evolution $\bar{J}(t)$ for a relative density $R = 0.05$ as compared to its approximation by a power function of At^n. The later proves to be slow time dependent with a low power coefficient $n = 0.0741$.

Since macroscopic creep compliance and relaxation modulus are related in Laplace transform by:

$$\int_0^t \bar{J}(t-\tau)\bar{E}_R(\tau)d\tau = t \tag{5}$$

The creep compliance and relaxation modulus are inverse for the initial and long time:

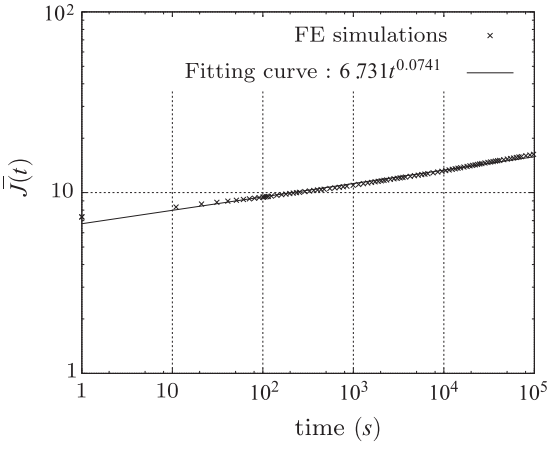

Figure 3. Effective creep compliance predictions of relative density $R = 0.05$.

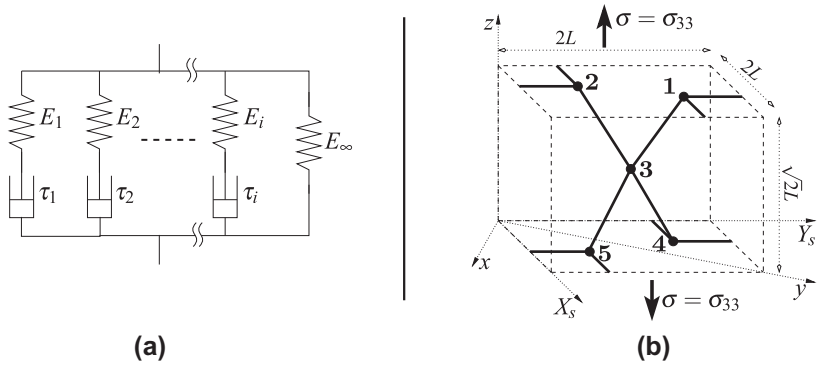

Figure 4. (a) Rheological model for the strut's material; (b) RVE under tensile stress.

$$\bar{J}(0)\ \bar{E}_R(0) = 1 \qquad \text{and} \qquad \bar{J}(\infty)\ \bar{E}_R(\infty) = 1 \tag{6}$$

For times between these extremes and a creep compliance variation represented by a power function of time:

$$\bar{J}(t) = At^n \tag{7}$$

the relaxation modulus yields Findley, Lai, and Onaran (1976):

$$\bar{E}(t) = \frac{1}{\bar{J}(t)}\,\mathscr{F}(n) \qquad \text{with} \qquad \mathscr{F}(n) = \frac{\sin(n\pi)}{n\pi} \tag{8}$$

For slow time dependence creep compliance function ($n \to 0$ in (7)), (8) leads to $\mathscr{F}(n) \to 1$ and an approximated simple inversion relation can be deduced between the creep compliance and the relaxation modulus:

$$\bar{E}_R(t) \simeq 1/\bar{J}(t) \tag{9}$$

This approximation is valid when the variation of creep compliance is slow over time (Figure 3). The FE macroscopic relaxation modulus is then deduced by combining (9) and (4).

3. Micromechanical model

Several studies tried to find a link between microscopic and macroscopic properties of foams by using beam models as a scale transition Gibson (2005), Zhu et al. (1997), Warren and Kraynik (1997), Li et al. (2003). Among the unit cells used in literature and regarding the microstructural investigation presented in introduction, we will focus on the model of tetrakaidecahedron cells packed in a BCC lattice which is well appropriate for PU open-cell foams. As illustrated in Figure 1(b), the tetrakaidecahedron cell contains six square and eight hexagonal faces and is created by truncating the corners of a cube. Consider a coordinate system (xyz) whose axes are parallel to the truncated cube axes, whereby the BCC lattice possesses cubic orthotropy and could be periodically extended in the three orthogonal directions. The Young's moduli in the

lattice vector directions are equal, so only one needs to be evaluated. In order to calculate the homogenised Young's modulus in the z direction $\bar{E}_{zz}$, a pair of tensile stress σ is applied in the z-direction as shown in Figure 4(b). The homogenised Young's modulus is then simply noted by $\bar{E}$. Regarding the mirror symmetry of the loading and geometry on dashed outlines of planes in Figure 4(b), we define a representative volume element (RVE) cell bounded by the symmetry planes (let $(X_s Y_s Z_s)$ be the coordinate system of RVE cell structure).

All the struts of the tetrakaidecahedron cell are assumed to be uniform, elastic and isotropic (of Young's modulus E) beams satisfying the classical beam theory. The relative density R is defined in Section 2 (Equation (1)).

3.1. Elastic behaviour

Our calculation is based on the general Cosserat homogenisation framework presented in Onck (2002). This concept is based on the idea of considering the translational and rotational degrees of freedom of material particles as independent variables. The material description is then defined by the couple stresses in addition of the ordinary Cauchy stresses. The Cosserat model is used in description of complex microstructure like granular and powder material, cellular media, bones and foams. For open-cell foams, the microstructure can be considered as a system of elastic beams where the force and couple interaction is essential. By taking into account these rotational degrees of freedom, the homogeneous medium inherits the couple stress properties of the constituted beam system. The transition from the microscopic scale to macroscopic one is detailed in Onck (2002) and resumed in the context of pen cell foams.

Each material point of the macroscopic continuum body is seen as the centre of a RVE (volume V) made of a cellular material. The macroscopic stress σ_{ij} is transmitted to the cellular RVE through local forces at the RVE's boundary:

$$f_i^{(k)} = \sigma_{ij}\, n_j^{(k)}\, ds^{(k)} \tag{10}$$

where $f_i^{(k)}$ is the force acting on node (k) associated with surface area $ds^{(k)}$ and $n_j^{(k)}$ the unit vector normal to surface $ds^{(k)}$. We solve the equilibrium problem on a micromechanical scale by determining displacements. The computation of equivalent macroscopic deformation uses an energetic equivalence between the average external work on the discrete material sample $\bar{W}$ and the strain energy density W in the macroscopic material point:

$$\bar{W} = \frac{1}{V}\sum_k f_i^{(k)}\, u_i^{(k)} \quad \equiv \quad W = \frac{1}{2}\,\sigma_{ml}\varepsilon_{ml} \tag{11}$$

where $u_i^{(k)}$ the node displacement due to the force acting $f_i^{(k)}$ and ε_{ml} the effective macroscopic strain measure identified as:

$$\varepsilon_{ij} = \frac{1}{V}\sum_k \frac{1}{2}\left(n_j^{(k)} u_i^{(k)} + n_i^{(k)} u_j^{(k)}\right)\, ds^{(k)} \tag{12}$$

Considering the symmetry of the base tetrakaidecahedra cell and sitting on a BCC lattice (Figure 4(b)), we define a new coordinate system (XYZ) related to the edges with unit vectors $(i,j,k)_{XYZ}$ which are related to those of the BCC lattice $(e_1, e_2, e_3)_{xyz}$ by:

$$i = e_1;\ j = \frac{1}{\sqrt{2}}e_2 - \frac{1}{\sqrt{2}}e_3 \quad \text{and} \quad k = \frac{1}{\sqrt{2}}e_2 + \frac{1}{\sqrt{2}}e_3 \tag{13}$$

Regarding the large web radius at the junction between edges, it will be assumed in this calculation that there is no vertex distorsion.

Using the notation of Figure 4(b), the effective macroscopic strain ε_{33} reads:

$$\varepsilon_{33} = \frac{1}{V}\sum_k \left(n_3^{(k)}\ u_3^{(k)}\ ds^{(k)}\right) \tag{14}$$

Within this tensile test, the nodes subjected to extension force $f^{(k)}$ are 1, 2, 4 and 5. We attach to each node (k) an elementary area $ds^{(k)}$ (w.r.t. the force equilibrium (10)): $ds^{(1)} = ds^{(2)} = ds^{(4)} = ds^{(5)} = 2L^2$. Substituting in (14) and noting that the node absolute displacement is the same, the effective macroscopic strain ε_{33} leads to:

$$\varepsilon_{33} = \frac{1}{4\sqrt{2}L}(8\ u_3^{(1)}) \tag{15}$$

where the only displacement component $u_3^{(1)}$ needs to be determined.

Using the force equilibrium $f_3^{(1)} = \sigma_{33}\ n_3^{(1)}\ ds^{(1)} = 2\sigma L^2$ and projecting into the (XYZ) coordinate system gives:

$$f^{(1)} = {}^t(0,\ 0,\ 2\sigma L^2)_{xyz} = {}^t(0,\ F_Y,\ F_Z)_{XYZ} \quad \text{with} \quad F_Z = -F_Y = \frac{2\sigma L^2}{\sqrt{2}} \tag{16}$$

As we suppose that the rotation of node 1 relative to node 3 about the X axis is zero, it follows from equilibrium of moments that $M_X = -\frac{F_Z L}{2}$.

Making use of the principle of superposition, one may check that:

$$u^{(1)} = {}^t\left(0,\ \frac{F_Y L}{AE},\ \frac{F_Z L^3}{12EI}\right)_{XYZ} \tag{17}$$

Substituting (16) in (17) and projecting into coordinate system (xyz), the displacement of node 1 in the z direction reads:

$$u_3^{(1)} = \sigma\left(\frac{L^3}{AE} + \frac{L^5}{12EI}\right) \tag{18}$$

and finally, using (15), the homogenised Young's modulus in the z direction $\bar{E}_{zz}$ yield:

$$\bar{E} = \bar{E}_{zz} = \frac{\sigma}{\varepsilon_{33}} = \chi\ E \quad \text{with} \quad \chi = \frac{6\sqrt{2}I}{L^4\left(1 + \frac{12I}{AL^2}\right)} \tag{19}$$

χ is a constant depending on the geometrical microstructure parameters.

A similar work can be conducted for the homogenised Poisson's ratio:

$$\bar{\nu} = -\frac{\varepsilon_{22}}{\varepsilon_{33}} = \frac{1AL^2 - 12I}{2AL^2 + 12I} \tag{20}$$

This result shows explicitly the dependence of the effective mechanical properties on the foam density R, the elastic properties of the constitutive material and the edge cross section shape which is characterised by the length L of each edge, the cross-sectional area A and the second moment of area I. For square sections with side a, $A = a^2$ and $I = a^4/12$. Using (1), the homogenised Young's modulus (19) and Poisson's ratio (20) for square sections edge reads:

$$\bar{E} = \frac{4\sqrt{2}R^2}{9 + 12\sqrt{2}R}E \quad \text{and} \quad \bar{\nu} = \frac{3 - 4\sqrt{2}R}{6 + 8\sqrt{2}R} \tag{21}$$

It is worth noting that this result is identical to that obtained by Zhu et al. (1997) using an energetic method. This result is also close to that of Li et al. (2003) which used Castigliano's energy. Its analysis is performed on a tertrakaidecahedral unit cell and the expressions of Young's modulus and Poisson's ratio are, respectively:

$$\begin{aligned} \bar{E} &= \frac{c\ R^2}{0.0787 + (1.1719 + 1.2187k(1+\nu)cR}E \\ \bar{\nu} &= \frac{0.3421 + 0.2977(1 + 6(1+\nu)k)cR}{1 + 0.5955(25 + 26(1+\nu)k)cR} \end{aligned} \tag{22}$$

where $c = I/A^2$ and k are two geometric parameters which depend on the shape of the edge's section. For square sections, $c = 0.0833$ and $k = 1.2$.

3.2. *Viscoelastic behaviour using Laplace Carson Transform (LCT)*

At small strains, open cellular materials have a linear viscoelastic response. In other words, creep strains are proportional to the stress under a constant load at any given time. Therefore, by taking advantage of the correspondance principle, we will employ the elastic solutions for solving linear viscoelastic behaviour. The macroscopic viscoelastic behaviour of cellular materials will be defined in terms of effective relaxation moduli and equivalently creep compliances using the microscopic ones and the geometric properties. For a homogeneous linear viscoelastic solid, the three-dimensional constitutive equation is given by Boltzmann's superposition principle as follows:

$$\boldsymbol{\sigma}(t) = \int_{-\infty}^{t} \mathbb{C}(t-\tau) : \dot{\boldsymbol{\varepsilon}}(\tau) d\tau \tag{23}$$

where $\mathbb{C}(\tau)$ is the fourth order viscoelastic relaxation tensor and $\dot{\mathbf{e}}$ is the second order strain rate tensor.

The viscoelastic strut material's behaviour obey the relaxation law presented in Section 2.2 (Equation (3)).

Using the LCT, the viscoelastic response can be written as the elastic solution when a change of variables is made. The following correspondence relates the elastic constants to the relaxation functions in the Laplace Carson domain (Salençon, 1983): $E \leftrightarrow s\ E_R(s)$. Subsequently, we apply this methodology to extend the effective elastic

moduli obtained in Section 3.1 to linear viscoelastic behaviour. Since the effective elastic moduli is linear w.r.t. the strut moduli, the application is found to be simple. As we apply the correspondance principle on elastic solution given by Equation (19), we have in Laplace–Carson domain:

$$s\,\bar{E}_R(s) = \chi\; s\; E_R(s) \quad \text{with} \quad \chi = \frac{6\sqrt{2}I}{L^4\left(1+\frac{12I}{AL^2}\right)} \tag{24}$$

Appling Laplace transform, (24) then yield:

$$d\,\bar{E}_R(t) = \chi\; d\; E_R(t) \quad \Rightarrow \quad \int_0^t d\,\bar{E}_R(\tau) = \chi \int_0^t d\; E_R(\tau) \tag{25}$$

where it was assumed that the material has been stress free for times anterior to zero. Considering that $\bar{E}_R(+\infty) = \bar{E}$ and using the relationship between $\bar{E}$ and E (19), we obtain:

$$\bar{E}_R(t) = \chi\; E_R(t) \tag{26}$$

This means that, as well as the elastic behaviour, the foam's relaxation is also linearly related by the ratio χ to the one of the constitutive solid and that it is sufficient to replace the elastic modulus by the time-dependent relaxation function. A similar result was founded by Huang and Gibson (1991) who, starting from the proportionality between the elastic constants of the open-cell foams and an empirical equation describing the viscoelastic behaviour of solid polymer, ended with a relative creep compliance of the foam: $\bar{J}(t) = (E/\bar{E})\; J(t)$. Micromechanical foam model of Li et al. (2003) (22) is also generalised, by means of LCT, to linear viscoelasticity.

4. Application to PU foams

A Bulpren PU open-cell foam is considered as an application to compare predictions of elastic constants given by FE simulation (Section 2.1) and analytical model (Section 3.1). The constitutive material of the solid skeleton is considered as an

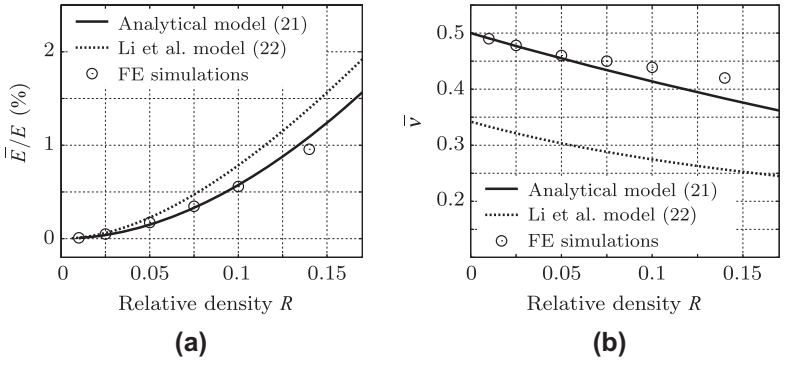

Figure 5. Effective properties of a foam w.r.t. the relative density: (a) normalised Young's modulus, (b) Poisson's ratio.

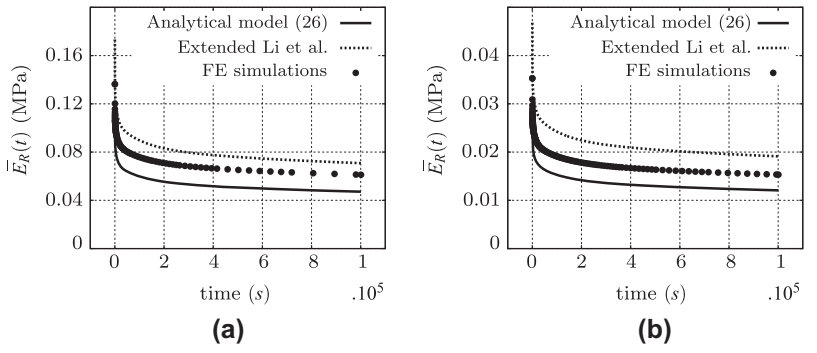

Figure 6. Effective relaxation modulus predictions of polymer foams: (a) Polymer foam of relative density 0.05; (b) Polymer foam of relative density 0.025.

isotropic solid characterised by Young's modulus $E = 100\ MPa$ and Poisson's ratio $v = 0.45$. The variation of foam's Young's moduli and Poisson's ratio predicted by the homogenisation models (Equations (21) and (22)) w.r.t. relative density R (1) is plotted in Figure 5, along with FE results.

It is seen in Figure 5(a) that at low relative densities, all predictions of Young's modulus are close. For higher densities, the model based on the Cosserat homogenisation framework, which is coincides with the Zhu et al. (1997) prediction, gives a good agreement with FE and the difference with Li et al. (2003) predictions increases with relative density. As shown in Figure 5(b), despite the fact that the analytical models emanate from the same idealised microstructure (tetrakaidecahedral cell), there is an unexpected difference between the Poisson's ratios predicted by each one. For lower relative densities, Poisson's ratio predicted by Cosserat homogenisation framework comes close to 0.5 and, therefore, an incompressible behaviour. This result agrees well with that obtained by FE simulations.

For the viscoelastic behaviour, we compare the effective relaxation modulus obtained by FE simulation (Section 2.2) and analytical model (Section 3.2). The viscoelastic strut material's stress relaxation data are approximated by the rheological model described in Section 2.2 (Figure 4(a)). The rheological model parameters (Equation (3)) are identified using the experimental data obtained by Zhu and Mills (2006) on solid Bulpren PU. They approaximated the relaxation Young's modulus with eight relaxation times $\tau_i = 10^{\,i-3}$ of moduli $E_i = 9.3$ MPa for $i = 1$ to 8 and $E_\infty = 28$ MPa.

We report in Figure 6 the different predictions of the effective relaxation modulus from different models confronted to FE computations for polymer foams having, respectively, 0.05 and 0.025 of relative density. As depicted in Figure 6, FE results are bounded by the analytical predictions.

5. Conclusion

In the first part of this paper, microstructural description of the open-cell foams is presented. Based on the cell micro-architecture, FE model is performed on a unit cell under periodic boundary conditions in order to compute the macroscopic elastic and viscoelastic behaviour. Then, a micromechanical model using Crosserat homogenisation framework was conducted to predict the properties of open-cell foams. Analytical model was developed and assessed by comparing them to FE computations. The macro-

scopic elastic behaviour was found to be linearly dependent to the elastic properties of the strut material. This proportionality depends on both the shape of the edges and the relative density of the foam. For the low relative density, the analytical predictions of Young's modulus and Poisson's ratio was close to those of FE, but small discrepancy was observed with increasing relative density particularly for the Li et al. (2003) model.

Elastic solutions were extended to linear viscoelasticity using LCT. The macroscopic relaxation function follows the same proportional factor that of the elastic behaviour; the elasticity of the strut material is simply replaced by its relaxation function. The analytical results have been compared with the Li et al. (2003) model (extended to viscoelasticity via LCT) and FE computations.

It is worth mentioning that while we modelled open-cell cellular solids by a periodic model, the real material is random and its microstructure is more complex. The limitation of previously discussed models is that they do not account for the natural irregularities due to imperfect geometry or/and irregular arrangement of cells. This is out of the scope of the current study, for a thorough analysis of the effect of cell irregularities on the overall mechanical behaviour, refer for instance to Li, Gaon and Subhash (2006) and Zhu, Hobdell and Windle (2000).

References

Bornert, M., Bertheau, T., and Gilormini, P. (2001). Homogenization in mechanics of materials 1. Hermes Science Publications.

Findley, W. N., Lai, J. S., & Onaran, K. (1976). *Creep and relaxation of nonlinear viscoelastic materials*. New York: Dover.

Gibson, L. J. (2005). Biomechanics of cellular solids. *Journal of Biomechanics, 38*, 377–399.

Huang, J. S., & Gibson, L. J. (1991). Creep of polymer foams. *Journal of the Mechanics and Physics of Solids, 26*, 637–647.

Li, K., Gao, X. L., & Roy, A. K. (2003). Micromechanics model for three-dimensional open-cell foams using a tetrakaidecahedral unit cell and Castiglianos second theorem. *Composites Science and Technology, 63*, 1769–1781.

Li, K., Gaon, X.-L., & Subhash, G. (2006). Effets of cell shape and strut cross-sectional area variation on the elastic properties of three-dimensional open-cell foams. *Journal of the Mechanics and Physics of Solids, 54*, 783–806.

Magnenet, V., Rahouadj, R., Bacher, P., & Cunat, C. (2008). Inelastic constitutive relations for foamed materials: A statistical approach and its application to open-cell melamine. *Mechanics of Materials, 40*, 673–684.

Mills, N. J. (2006). Finite element models for the viscoelasticity of open-cell polyurethane foam. *Cellular polymers, 25*(5), 296–316.

Onck, P. R. (2002). Cosserat modeling of cellular solids. *Comptes Rendus Mécanique, 330*, 717–722.

Roberts, A. P., & Garboczi, E. J. (2002). Elastic properties of random three-dimensional open cell solids. *Journal of the Mechanics and Physics of Solids, 50*, 33–55.

Salençon, J. (1983). Viscoelasticity. Paris: Presses de l'ENPC.

Warren, W. E., & Kraynik, A. M. (1997). Linear elastic behavior of a low-density Kelvin foam with open cells. *Journal of Applied Mechanics, 64*, 787–794.

Zhu, H. X., Hobdell, J. R., & Windle, A. H. (2000). Effects of cell irregularity on the elastic properties open-cell foams. *Acta Materialia, 48*, 4893–4900.

Zhu, H. X., Knott, J. F., & Mills, N. J. (1997). Analysis of the elastic properties of open cell foams with tetrakaidecahedral cells. *Journal of the Mechanics and Physics of Solids, 45*, 319–345.

Zhu, H. X., & Mills, N. J. (2006). Modelling the creep of open cell polymer foams. *Journal of the Mechanics and Physics of Solids, 47*, 1437–1457.